

A Semiconductor or A One-Dimensional Metal and Superconductor through Tellurium π Stacking**

Ejaz Ahmed, Johannes Beck,* Jörg Daniels, Thomas Doert, Steffen Jan Eck, Andreas Heerwig, Anna Isaeva, Sven Lidin, Michael Ruck,* Walter Schnelle, and Alexander Stankowski

Metallic behavior is a well-recognized feature of charge-transfer compounds that contain oxidized or reduced stacks of planar π -conjugated molecules. Electronic conduction takes place in the partially occupied π bands formed by intermolecular orbital overlap. Some of these materials even exhibit superconductivity.^[1] Tetrathiofulvalene–tetracyanoquinomethane (TTF–TCNQ) was the first compound with enhanced conductivity ($\sigma(300\text{ K}) = 10^5\text{ }\Omega^{-1}\text{ m}^{-1}$) owing to the charge transfer between separate stacks of the TTF cations (charge donors) and TCNQ anions (charge acceptors). These impressive transport characteristics persist down to about 54 K, at which temperature the compound undergoes a metal–insulator transition owing to a Peierls distortion.^[2] In the first organic superconductor, (TMTSF)₂PF₆ (TMTSF = tetramethyl-tetraselenafulvalene),^[3] the low-temperature metal–insulator transition could be suppressed by hydrostatic pressure. A series of charge-transfer salts, named after Bechgaard and composed of segregated stacks of planar TMTSF donors and monovalent anion acceptors with the general formula (TMTSF)₂X (X = PF₆[−], AsF₆[−], TaF₆[−], SbF₆[−], NbF₆[−], ClO₄[−], or ReO₄[−]), has been produced. Transition temperatures (T_c) of 1–2 K have been reported for the Bechgaard salts, with only the X = ClO₄[−] compound showing superconductivity at ambient pressure.

To date, examples of purely inorganic π systems demonstrating electronic conduction are quite rare; the intermetallic compounds BaE₃ (E = Sn,^[4a] Ge^[4b]) show superconductivity below about 4 K, which is attributed to the interactions in ¹[E₃]^{2−} stacks.

Herein we present two new main-group salts, Te₄[Bi_{0.67}Cl₄] (1) and Te₄[Bi_{0.74}Cl₄] (2), both exhibiting columnar structures of square tellurium polycations Te₄^{(2− δ)+} alternating with stacks of chloridobismuthate(III) polyhedra (Figure 1). The electron-precise compound 1 ($\delta = 0$) shows the conductivity characteristics of a semiconductor (estimated band gap

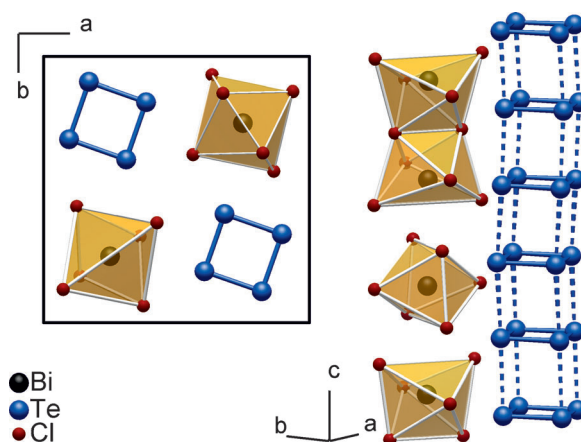


Figure 1. Sections of the incommensurately modulated structure of **2**. Left: Projection along the *c* axis. Right: Sequence of chloridobismuthate anions and stacks of tellurium polycations.

0.16 eV; $\sigma(300\text{ K}) = 50\text{ }\Omega^{-1}\text{ m}^{-1}$; Supporting Information, Figure S1) in a temperature range of 250–330 K, while the slightly Bi-rich 2 ($\delta = 0.22$) is an exceptionally good one-dimensional metallic conductor at room temperature ($\sigma(300\text{ K}) = 0.43 \times 10^6\text{ }\Omega^{-1}\text{ m}^{-1}$, depending on the pressure used to form the polycrystalline pellet). Moreover, **2** undergoes no Peierls distortion upon cooling but a sharp transition to a superconducting state at 7.15 K, which is an unprecedentedly high T_c for a π -stack conductor at ambient pressure (Figure 2). The very small difference between field cooling and zero-field cooling susceptibilities hints at a type I superconductor. The bulk character of the superconducting phase was confirmed by specific heat and further magnetization measurements.^[5] Above T_c , Pauli paramagnetism superimposed by strong diamagnetism is observed. The linear temperature dependence of the susceptibility even to low temperature indicates a very low defect concentration (Supporting Information, Figure S2).

The two compounds were synthesized by different routes. Compound **1** was obtained by chemical vapor transport (CVT) at a deposition temperature of 400 K, whereas **2** was isolated from an ionic liquid (IL) [BMIM]Cl/AlCl₃

[*] Dr. E. Ahmed, Prof. Dr. T. Doert, Dr. A. Heerwig, Dr. A. Isaeva, Prof. Dr. M. Ruck
Department of Chemistry and Food Chemistry
Technische Universität Dresden
01062 Dresden (Germany)
E-mail: michael.ruck@tu-dresden.de

Dr. E. Ahmed, Prof. Dr. M. Ruck, Dr. W. Schnelle
Max-Planck-Institut für Chemische Physik fester Stoffe
Nöthnitzer Strasse 40, 01187 Dresden (Germany)
Prof. Dr. J. Beck, Dr. J. Daniels, Dr. S. J. Eck, Dr. A. Stankowski
Department of Inorganic Chemistry, Universität Bonn
53121 Bonn (Germany)
E-mail: j.beck@uni-bonn.de

Prof. Dr. S. Lidin
Division of Polymer & Materials Chemistry, Lund University
22100 Lund (Sweden)

[**] This work was supported by the Higher Education Commission of Pakistan (HEC) and the Deutsche Forschungsgemeinschaft (DFG).

Supporting information for this article is available on the WWW under <http://dx.doi.org/10.1002/anie.201200895>.

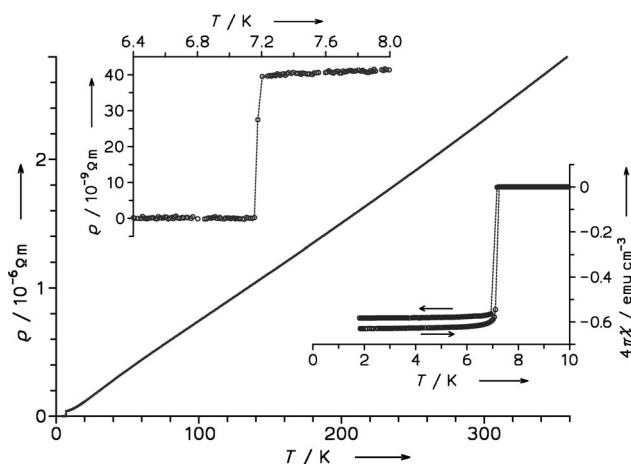


Figure 2. Temperature dependence of the electrical resistivity of a cold-pressed bar of **2**. Upper inset: magnification of the main curve at low temperatures. Lower inset: magnetic volume susceptibility of **2** (as prepared) in an external field $\mu_0 H = 2$ mT.

([BMIM]⁺ = 1-*n*-butyl-3-methylimidazolium) at room temperature. The reactions can be interpreted as the synproportionation of elemental tellurium and tellurium(IV) to a low-valent intermediate facilitated by the Lewis acid BiCl₃, which accepts chloride ions from TeCl₄. The CVT technique is nowadays considered to be a conventional method, whereas the IL-based synthesis is an emerging but extremely fruitful approach.^[6] Further synthetic routes, using various media, towards semiconducting compounds that contain polycationic species of tellurium in isolated or polymeric forms have also been established.^[7] We have observed by X-ray single-crystal diffraction and EDX analysis that a specific synthetic setup results in the reproducible formation of a single-phase product with a certain Bi content.

The minimal structural differences between **1** and **2** manifest themselves in two types of superstructural ordering. In both cases, low-intensity satellite reflections indicate incommensurately modulated structures (Supporting Information, Figure S3,S4). The subtle but essential discrepancy lies in the centering of the superstructure and, of course, in the significantly different bismuth content. As the crystal quality of **2** is clearly superior to that of **1**, we focus on the room-temperature structure of **2** in the following: Bi and Cl atoms form a complex sequence of anions with average composition [Bi_{0.74}Cl₄]^{1.78-}, while the Te atoms constitute slightly distorted square polycations, which are stacked ecliptically parallel to the *c* axis. In the projection along the *c* direction, a checkerboard pattern of both structural motives results (Figure 1). In the course of the occupancy modulation of the Bi atoms, the positions of the Cl atoms vary markedly, which leads to a strong modulation of the Bi–Cl distances (Supporting Information, Table S5, Figure S5–S8). Along [001], isolated [BiCl₆]³⁻ and [Bi₂Cl₁₀]⁴⁻ groups form an aperiodic sequence. The Cl atoms at the edges of neighboring groups define empty tetrahedra. Similar sequences have been observed in [Bi₃Ni]₂[Bi_{1-δ}Br_{4(–2δ)}]Br and [PdBi₆][(Bi₃Sn)_{1-δ}Br_{4-δ}]Br.^[8] From this perspective, **1** and **2** can be classified “misfit stack compounds”.

The described modulations provide a degree of freedom for the Bi content and thereby a variable electron count: the tellurium stack of **2** is slightly more reduced. Disregarding electrostatic repulsion, the tellurium polycations are stacked ecliptically in both compounds; this structural peculiarity can only be rationalized by assuming attractive forces between rings that exceed π -stacking interactions known from mainly uncharged aromatic systems. The competition of intra- and inter-ring bonding seems to account for decisive changes in electron conduction.

Square-planar Te₄²⁺ polycations are well-known, and typical bond lengths from 265 to 270 pm have been reported.^[9] The chemical bonding in the isolated Te₄²⁺ polycation has been described by bonding MOs composed of 5p_x and 5p_y atomic orbitals and an aromatic π -binding system created by the 5p_z orbitals (Figure 3).^[10] In total, a bond order of 1.25 per Te–Te interaction results. The calculated electron count in this bonding region (electron localizability indicator (ELI-D) formalism)^[11] yields 1.44 electrons.

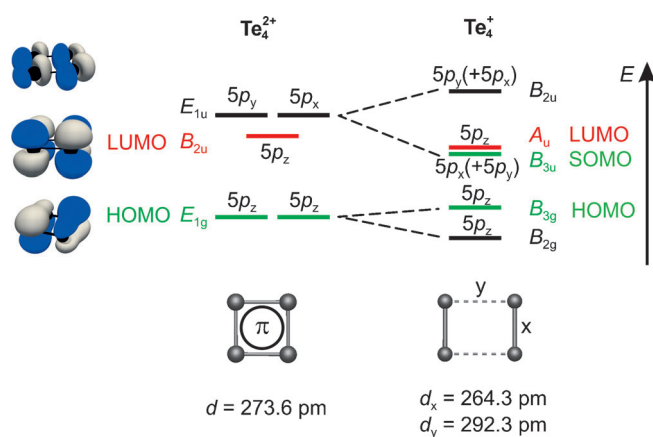


Figure 3. Semiquantitative energy schemes of the highest occupied states in the square Te₄²⁺ polycation and the equilibrium structure of a hypothetical Te₄⁺. For complete MO diagrams, see the Supporting Information, Figure S9.

Because of the modulation, each Te₄ ring in **1** and **2** deviates individually from *D*_{4h} symmetry. In **1**, the Te–Te interatomic distances are found in a wide range from 248(3) to 299(3) pm, with an average of 275 pm. In contrast, the bond lengths in **2** vary only in the narrow range from 274.8(3) to 275.9(3) pm, with an average of 275.3(4) pm (Supporting Information, Table S5, Figure S7). Thus, apart from the irregular distortion, an overall lengthening of interatomic distances can also be stated. The distances between adjacent rings in the stack range from 328 to 410 pm in **1** and from 351 to 357 pm (average 352.4(1) pm) in **2**, which is clearly less than the sum of the van der Waals radii of 412 pm for Te.^[12]

In the case of **1**, the ionic formula Te₄²⁺[Bi_{0.67}Cl₄]²⁻ = (Te₄)₃[Bi₂Cl₁₂] represents the electron-precise system and corresponds with the observed semiconducting properties. In **2**, the Te₄²⁺ polycations are partially reduced (average charge +1.78). The optimized geometry of a hypothetical isolated

Te_4^+ has D_{2h} symmetry and represents a rectangle with a shortened bond along x (264 pm) and an elongated bond along y (292 pm). The distortion of the molecule comes along with the splitting of the antibonding $19E_{1u}$ MO of the Te_4^{2+} into two MOs. One of them ($19B_{3u}$) is lowered in energy and becomes the SOMO of the Te_4^+ unit (Figure 3). In accordance with lifted degeneracy of the formerly nonbonding $19E_{1u}$ MO, the π bonding along the edge x of Te_4^+ is enhanced (bonding ELI-D basin contains 1.57 electrons), whereas bonding along y is weakened (ELI-D basin population: 0.26 electrons). Such a dramatic rectangular distortion has been observed in $[\text{Et}-\text{Te}-\text{Te}-\text{Et}]_2^{2+}(\text{CF}_3\text{SO}_3^-)_2$,^[13] however, it does not occur in the room-temperature structure of **2**.

The reason is the competition of the intramolecular in-plane bonding with intermolecular bonding perpendicular to the molecular plane, which employs the same MOs composed of $5p_z$ AOs to form the conduction band (Supporting Information, Figure S10). The band dispersion along the c^* direction (Γ –Z) increases when the inter-ring distance becomes shorter. Below a critical distance, band states evolving from the LUMO of the undistorted Te_4^{2+} ring are lower in energy than the SOMO of the distorted Te_4^+ ring. As a consequence, additional electrons fill the band states instead of the in-plane localized states, and the distortion of the reduced tellurium rings vanishes. In fact, the calculated band structure (DFT, TB-LMTO-ASA) of **2**, that is, the compound with equidistant and almost square Te_4 rings, shows bands formed by $\text{Te}5p$ orbitals that cross the Fermi level in the direction of the eclipsed stacking (Supporting Information, Figure S10). The entire band structure is the fingerprint of a one-dimensional metal. Furthermore, co-existence of flat bands along the Γ –X–M– Γ directions (the ab plane) with the steep bands in the Γ –Z direction (along the stacks) is in accordance with the scenario defined as a prerequisite for superconductivity by Simon et al.^[14]

On the other hand, the calculations suggest (Supporting Information, Figure S11) that the metallic conductivity along the c axis can be effectively hindered upon the Te_4 ring distortion. Further investigations on the structures and the physical properties are in progress to verify this preliminary interpretation. It will be worth doing so in view of the exceptionally efficient 1D conductivity at room temperature and the superconductivity with yet unknown mechanism and much higher T_c than in Bechgaard salts.

Experimental Section

Synthesis by CVT: $\text{Te}_4[\text{Bi}_{0.67}\text{Cl}_4]$ (**1**) was obtained in ca. 10% yield by reacting a mixture in the molar ratio of Te, TeCl_4 , and BiCl_3 of 5:2:1 in a fused evacuated glass ampoule ($l=120$ mm, $d=12$ mm). The ampoule was heated in a temperature gradient from 468 K to 403 K. Within a week, air-sensitive golden lustrous needles deposited at the colder side of the ampoule (Supporting Information, Figure S12). After prolonged annealing, the crystals of **1** disappear and the neighboring phases $\text{Te}_4[\text{Bi}_{0.20}\text{Cl}_{20}]$, $\text{Te}_8[\text{Bi}_4\text{Cl}_{14}]$, and $(\text{Te}_4)(\text{Te}_{10})$ – $[\text{Bi}_4\text{Cl}_{16}]$ ^[15] are formed. Although the EDX analysis was hampered by high air- and moisture sensitivity, the compounds **1** and **2** were distinguishable. Calculated composition of **1** [atom %]: 46.15 (Te), 7.69 (Bi), 46.16 (Cl); experimental composition (EDX, DSM 940, Zeiss): 44.91 (Te), 7.70 (Bi), 47.39 (Cl).

Synthesis in IL: The starting materials were handled in an argon-filled glove box (M. Braun; $p(\text{O}_2)/p^0 < 1$ ppm, $p(\text{H}_2\text{O})/p^0 < 1$ ppm). Golden lustrous needles of $\text{Te}_4[\text{Bi}_{0.74}\text{Cl}_4]$ (**2**) were obtained in high yield by reacting a stoichiometric mixture of Te (99.999%, Fluka), TeCl_4 (99.9%, Strem, twice-sublimated), and BiCl_3 (Alfa Aesar, anhydrous, 99.999%, sublimated three times) in an IL composed of $[\text{BMIM}]\text{Cl}$ (Merck, 98%) and AlCl_3 (Fluka, anhydrous, 98%, sublimated three times; molar ratio = 1:1.5) in a standard Schlenk tube (25 mL). The reaction mixture was left to stir overnight at room temperature and then filtered to remove the unreacted material. After two days, air-sensitive crystals formed. The excess IL was decanted in an argon-filled glove box, and single crystals were separated by washing in dry dichloromethane to remove any traces of IL. The yield of $\text{Te}_4[\text{Bi}_{0.74}\text{Cl}_4]$ (**2**) was 63%, and the compound was always exclusively obtained from ionic liquids. Calculated composition of **2** [atom %]: 45.77 (Te), 8.46 (Bi), 45.77 (Cl); experimental composition (EDX, DSM 940, Zeiss): 45.46 (Te), 8.63 (Bi), 45.91 (Cl).

X-ray diffraction of **1**: Tetragonal, superspace group $X4(00\gamma)q0$ ^[16] with $\gamma=0.555$; $a=1702.35(12)$, $c=702.85(5)$ pm; $V=2036.9(2) \times 10^6$ pm³; $Z=2$; $\rho_{\text{calc}}=5.24$ g cm^{−3}; imaging-plate diffraction system IPDS-II (Stoe), graphite-monochromated $\text{MoK}\alpha$ radiation ($\lambda=71.073$ pm); numerical absorption correction^[17,18] $\mu(\text{MoK}\alpha)=24.5$ mm^{−1}; 203 613 measured, 21 010 unique reflections, $R_{\text{int}}=0.21$, $R_o=0.15$; structure solution with charge flipping algorithm^[17,19] six harmonic modulation waves for the positional modulation of the Te atoms four harmonic waves for the positional modulations of the Cl atoms, composite model with Bi in second composite part $W2=\{1000\ 0100\ 002-1\ 001-1\}$ and six harmonic modulation waves for the positional modulation of the Bi atom and four harmonic waves for the occupational modulation of the Bi atom; 298 parameters (Supporting Information, Tables S1 and S2). For all reflections: R_1 [$4718\ F_o > 3\sigma(F_o)$] = 0.103, $R_1(\text{all } F_o)$ = 0.318, $wR_2(\text{all } F_o^2)$ = 0.225; for main reflections: R_1 [$1885\ F_o > 3\sigma(F_o)$] = 0.052, $R_1(\text{all } F_o)$ = 0.117, $wR_2(\text{all } F_o^2)$ = 0.130; for first-order satellites: R_1 [$1309\ F_o > 3\sigma(F_o)$] = 0.089, $R_1(\text{all } F_o)$ = 0.345, $wR_2(\text{all } F_o^2)$ = 0.212; for second-order satellites: R_1 [$747\ F_o > 3\sigma(F_o)$] = 0.281, $R_1(\text{all } F_o)$ = 0.532, $wR_2(\text{all } F_o^2)$ = 0.554; GooF = 1.69; residual electron density: approx. -3 to $+4\ e \times 10^{-6}$ pm^{−3} (Supporting Information, Figure S5). Site occupancy factor of Bi: 0.92(1); overall composition: $\text{Te}_4[\text{Bi}_{0.665(3)}\text{Cl}_4]$.

X-ray diffraction of **2**: Tetragonal, superspace group $P4/n(\frac{1}{2}\gamma)q0$ ^[16] with $\gamma=0.272(1)$; $a=1206.6(2)$, $c=352.4(1)$ pm; $V=513.0(2) \times 10^6$ pm³; $Z=2$; $\rho_{\text{calc}}=5.24$ g cm^{−3}; imaging-plate diffraction system IPDS-II (Stoe), graphite-monochromated $\text{MoK}\alpha$ radiation ($\lambda=71.073$ pm); numerical absorption correction^[17,18] $\mu(\text{MoK}\alpha)=24.8$ mm^{−1}; 16 420 measured, 1698 unique reflections, $R_{\text{int}}=0.112$, $R_o=0.026$; structure solution with charge flipping algorithm^[17,19] two harmonic modulation waves for the positional modulation of the Te and Cl atoms, crenel function for occupancy modulation of the Bi atom; 84 parameters (Supporting Information, Tables S3 and S4). For all reflections: R_1 [$759\ F_o > 3\sigma(F_o)$] = 0.031, $R_1(\text{all } F_o)$ = 0.094, $wR_2(\text{all } F_o^2)$ = 0.070; for main reflections: R_1 [$241\ F_o > 3\sigma(F_o)$] = 0.020, $R_1(\text{all } F_o)$ = 0.031, $wR_2(\text{all } F_o^2)$ = 0.048; for first-order satellites: R_1 [$394\ F_o > 3\sigma(F_o)$] = 0.035, $R_1(\text{all } F_o)$ = 0.072, $wR_2(\text{all } F_o^2)$ = 0.065; for second-order satellites: R_1 [$124\ F_o > 3\sigma(F_o)$] = 0.073, $R_1(\text{all } F_o)$ = 0.308, $wR_2(\text{all } F_o^2)$ = 0.135; GooF = 1.30; residual electron density: -2.03 to $+1.79\ e \times 10^{-6}$ pm^{−3}. Site occupancy factor of Bi: 0.370(1); overall composition: $\text{Te}_4[\text{Bi}_{0.740(1)}\text{Cl}_4]$.

Further details on the crystal structure investigations may be obtained from the Fachinformationszentrum Karlsruhe, 76344 Eggenstein-Leopoldshafen, Germany (fax: (+49) 7247-808-666; e-mail: crysdata@fiz-karlsruhe.de), on quoting the depository numbers CSD-424162 (**1**) and CSD-424133 (**2**).

For the quantum chemical calculations, see the Supporting Information.

Received: February 1, 2012

Revised: April 19, 2012

Published online: July 4, 2012

Keywords: ionic liquids · low-dimensional conductors · polycations · superconductivity · π -stacking interactions

- [1] a) M. R. Bryce, L. C. Murphy, *Nature* **1984**, *309*, 119–126; b) D. Jérôme, *Science* **1991**, *252*, 1509–1514; c) J. M. Williams, A. J. Schultz, U. Geiser, K. D. Carlson, A. M. Kini, H. H. Wang, W. K. Kwok, M. H. Whangbo, J. E. Schirber, *Science* **1991**, *252*, 1501–1508.
- [2] M. J. Cohen, L. B. Coleman, A. F. Garito, A. J. Heeger, *Phys. Rev. B* **1974**, *10*, 1298–1307.
- [3] a) K. Bechgaard, C. S. Jacobsen, K. Mortensen, H. J. Pedersen, N. Thorup, *Solid State Commun.* **1980**, *33*, 1119–1125; b) D. Jérôme, A. Mazaud, M. Ribault, K. Bechgaard, *J. Phys. Lett.* **1980**, *41*, L95–L98; c) K. Bechgaard, K. Carneiro, F. B. Rasmussen, M. Olsen, G. Rindorf, C. S. Jacobsen, H. J. Pedersen, J. C. Scott, *J. Am. Chem. Soc.* **1981**, *103*, 2440–2442.
- [4] a) T. F. Fässler, C. Kronseder, *Angew. Chem.* **1997**, *109*, 2800–2803; *Angew. Chem. Int. Ed. Engl.* **1997**, *36*, 2683–2686; b) H. Fukuoka, Y. Tomomitsu, K. Inumaru, *Inorg. Chem.* **2011**, *50*, 6372–6377.
- [5] W. Schnelle, E. Ahmed, M. Ruck, unpublished results.
- [6] a) E. Ahmed, M. Ruck, *Angew. Chem.* **2012**, *124*, 314–316; *Angew. Chem. Int. Ed.* **2012**, *51*, 308–309; b) E. Ahmed, M. Ruck, *Coord. Chem. Rev.* **2011**, *255*, 2892–2903; c) E. Ahmed, M. Ruck, *Dalton Trans.* **2011**, *40*, 9347–9357; d) D. Freudenmann, S. Wolf, M. Wolff, C. Feldmann, *Angew. Chem.* **2011**, *123*, 11244–11255; *Angew. Chem. Int. Ed.* **2011**, *50*, 11050–11060.
- [7] a) S. Brownridge, I. Krossing, J. Passmore, H. D. B. Jenkins, H. K. Roobottom, *Coord. Chem. Rev.* **2000**, *197*, 397–481; b) J. Beck, *Angew. Chem.* **1994**, *106*, 172–182; *Angew. Chem. Int. Ed. Engl.* **1994**, *33*, 163–172; c) J. Beck, *Coord. Chem. Rev.* **1997**, *163*, 55–70; Ref. [6b].
- [8] a) B. U. Wahl, T. Doert, T. Söhnle, M. Ruck, *Z. Anorg. Allg. Chem.* **2005**, *631*, 457–467; b) B. Wahl, M. Ruck, *Acta Crystallogr. Sect. B* **2009**, *65*, 593–599; c) B. Wahl, L. Kloo, M. Ruck, *Z. Anorg. Allg. Chem.* **2009**, *635*, 1979–1985.
- [9] a) T. W. Couch, D. A. Lokken, J. D. Corbett, *Inorg. Chem.* **1972**, *11*, 357–362; b) E. Ahmed, E. Ahrens, M. Heise, M. Ruck, *Z. Anorg. Allg. Chem.* **2010**, *636*, 2602–2606.
- [10] S. Schlüter, Doctoral Thesis, University of Bonn, Bonn **2004**.
- [11] a) M. Kohout, *Faraday Discuss.* **2007**, *135*, 43–54; b) M. Kohout, *Int. J. Quantum Chem.* **2004**, *97*, 651–658.
- [12] A. Bondi, *J. Phys. Chem.* **1964**, *68*, 441–451.
- [13] B. Müller, H. Poleschner, K. Seppelt, *Dalton Trans.* **2008**, *33*, 4424–4427.
- [14] a) A. Simon, *Angew. Chem.* **1997**, *109*, 1873–1891; *Angew. Chem. Int. Ed. Engl.* **1997**, *36*, 1788–1806; b) S. Deng, A. Simon, J. Köhler, *Angew. Chem.* **1998**, *110*, 664–666; *Angew. Chem. Int. Ed.* **1998**, *37*, 640–643.
- [15] a) J. Beck, M. Kasper, A. Stankowski, *Chem. Ber.* **1997**, *130*, 1189–1192; b) J. Beck, A. Stankowski, *Z. Naturforsch. B* **2001**, *56*, 453–457; c) J. Beck, A. Fischer, A. Stankowski, *Z. Anorg. Allg. Chem.* **2002**, *628*, 2542–2548.
- [16] L. Palatinus, G. Chapuis, *J. Appl. Crystallogr.* **2007**, *40*, 786–790.
- [17] a) V. Petříček, M. Dušek, L. Palatinus, *Jana2006, The Crystallographic Computing System*. Institute of Physics, Praha, Czech Republic, **2006**; b) V. Petříček, V. A. van der Lee, M. Evain, *Acta Crystallogr. Sect. A* **1995**, *51*, 529–535.
- [18] X-SHAPE, Crystal Optimisation for Numerical Absorption Correction Program, Version 1.06, Stoe & Cie GmbH, Darmstadt, **1999**.
- [19] a) A. Yamamoto, T. Janssen, A. Janner, P. M. de Wolff, *Acta Crystallogr. Sect. A* **1985**, *41*, 528–530; b) A. Yamamoto, *Acta Crystallogr. Sect. A* **1996**, *52*, 509–560.